International Journal of Current Engineering and Technology
E-ISSN 2277 – 4106, P-ISSN 2347 – 5161

Available at http://inpressco.com/category/ijcet

Research Article

Increasing the Speed of Polymer Injection Simulation in Hydrocarbon Reservoirs

Mehdi Foroozanfar#* and Mohammad Reza Rasaie!

#Department of Petroleum Engineering, Kish International Campus, University of Tehran, Iran
! Institute of Petroleum Engineering (IPE), School of Chemical Engineering, College of Engineering, University of Tehran, Iran

Received 05 Aug 2018, Accepted 08 Oct 2018, Available online 11 Oct, **Vol.8, No.5 (Sept/Oct 2018)**

Abstract

Reliable reservoir prediction is essential for optimized production and reservoir management. The prediction is normally done by reservoir simulation. Reservoir simulators solve fluid flow equations of reservoir numerically on homogenized coarse blocks of reservoir model. The original fine grids are generated by primary geological blocks which are output of geological software. The upscaling is necessary since geological software by means of statistical methods create models with millions and even billion of grid blocks and dynamic simulation on these models is practically not possible. We have performed an accurate and highly efficient method for upscaling and simulation of polymer injection in three-dimensional (3D) heterogeneous reservoir. In this study we introduced an upscaling method which inspired by nature, there are enough similar aspect between earth and hydrocarbon reservoir which can be used as a pattern for multi scale grid generation. This procedure done for polymer injection which is complex process with high computing volume. It generates a non-uniform grid in which the resolved structure of the fine grid around the wells, as well as in the high-permeability sectors, are preserved, but the rest of the grid is upscaled. The simulation results on the geological structure well compared with the results of upscaled models. The results confirm that nature-inspired method consumes less run time with nearly accuracy of fine model.

Keywords: *Polymer Flooding, Upscaling, Grid Modeling, Geological Model, Run Time*

1. Introduction

Recent amelioration in reservoir imaging techniques and geostatistical procedures allow very detailed reservoir explanations containing millions of grid blocks to be produced. However, time limitations in reservoir simulation generally limit the flow model to a coarser grid. Each coarse grid block property value is received from the original fine scale grid using different upscaling techniques.

After all averaging, interpolation and data populating, from a simulation point of view, geological models are ironically too complex and too large, i.e., they contain more information than we can handle in simulation studies. Therefore, we usually use a coarsened grid model, or a simulation flow model. The model contains of grid blocks with their petrophysical properties replaced by averaged or upscaled quantities based on variations of underlying geomodel quantities that occur at length scales below the simulation grid block. The main reason for using the upscaled models is computational limitations since it is usually impossible to perform flow simulations on the geomodel.

Significant progress was made when Durlofsky *et al*. (1997) introduced a method whereby finer resolution is used in the regions of high-fluid velocities, and upscaled, homogenized description is utilized for the rest of the domain. In their approach no upscaling scheme is used for the relative permeabilities, as the original rock curves are used for the upscaled grid blocks, hence making the technique process-independent.

Non-uniform grid coarsening offers significant computational speed-up and general applicability, but at the cost of increasing numerical dispersion and decreasing accuracy for the nonseparable scales. Such upscaling techniques are suitable for the sectors that are far from the wells. Since the pressure field in the near-well regions usually changes rapidly in the radial direction, the above upscaling approaches are not suitable. For such situations, well pseudo-functions to account for the pressure changes were suggested by Chappelear and Hirasaki (1976) and King *et al*. (1991). Durlofsky *et al*. (2000) developed a method for calculating the transmissibility and well index for single-phase flow based on the solution to the local well-driven flow. Grid selection methods that rely on dynamic responses, such as streamline simulation, in order to identify the locations of the grid blocks in the

*Corresponding author's ORCID ID:0000-0000-0000-0000
DOI: https://doi.org/10.14741/ijcet/v.8.5.11

geological model through which most of the fluids pass, were also proposed by Verma and Aziz (1996) and Castellini *et al*. (2000). Static methods, suggested by Garcia *et al*. (1992), Li and Beckner (2000), and Younis and Caers (2001, 2002), that rely on the spatial distribution of the permeability for developing upscaled grids, are also robust (Mohammad Reza Rasaei, Muhammad Sahimi,2007).

The objective of this paper is to define inspired by nature upscaling method and simulation of polymer injection for a 3D heterogeneous multiphase reservoir. Chemical enhance oil recoveries processes are extremely complex processes with very high computing volumes. The high amount of computations can increase simulation time. The scale enhancement method defined in this study is a nature-based approach whose performance is based on the behavior of the flow lines. It was able to scale-up three-dimensional heterogeneous reservoir by maintaining accuracy and increasing the speed of simulation. For upscaling multiphase flow, in addition to absolute permeabilities, relative permeabilities should be upscaled. Therefore, it is necessary to express the saturation equation in coarse scale. One way to write an upscaled saturation equation is by assuming that the functional form of these properties does not change with scale. In this case the same relative permeability and capillary pressure curves from fine to coarse scale are used. Unfortunately this suggestion fails in the presence of non-local heterogeneities similar to failure in the case of absolute permeability upscaling. In these circumstances, a multiphase upscaling technique is generally required (Barker & Thibeau, 1997). In this study, increasing the simulation speed is not only by reducing the number of blocks, but as the first step in choosing the method of solving the model among the methods IMPES, fully implicit and as solver methods and choose one of them based on minimum elapsed time and definition of upscaling methods for different terms like absolute permeability, relative permeability, transmissibility, pore volume are another segments of this paper.

2. Upscaling Pattern, Inspired by Nature (UPIN), Upscaling Pattern

The division of the Earth's surface is done by the latitude and longitude, this kind of division is the inspirational basis for increasing the scale.

- Latitude: Lines of latitude called parallels, measure distance north and south of equator.
- Longitude: Lines of longitude called meridians, measure distance east and west of prime meridian.

There are enough similar aspect between earth and hydrocarbon reservoir such as:

North Pole ≈ Production Well (Figure 1)
South Pole ≈ Injection Well (Figure 1)
Earth's Magnetic Field ≈ Streamline
Longitude ≈ Discretization in X Direction (Figure 2)
Latitude ≈ Discretization in Y Direction (Figure 2)

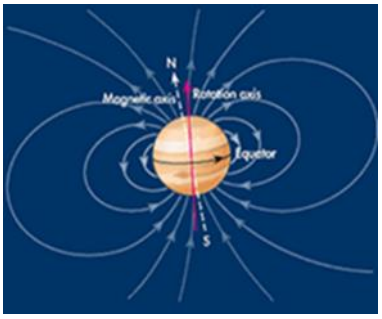

Figure 1: Earth's Magnetic Field

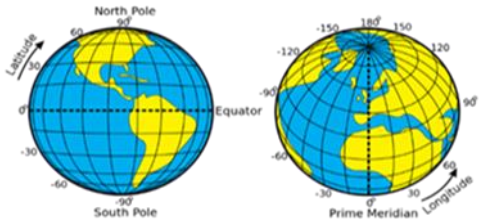

Figure 2: Latitude and Longitude

From south to the north pole the size of grid varies (figure 3):

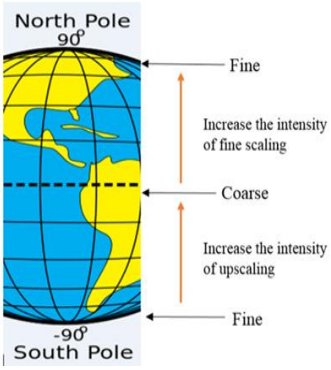

Figure 3: Grid Size

The earth's grid in the north and South Pole and in the equator is in the following form:

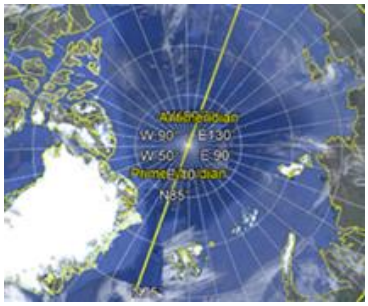

Figure 4: Earth's Grid in the North Pole (Fine-Scaled and Radial Form)

Figure 5: Earth's Grid in the South Pole (Fine-Scaled and Radial Form)

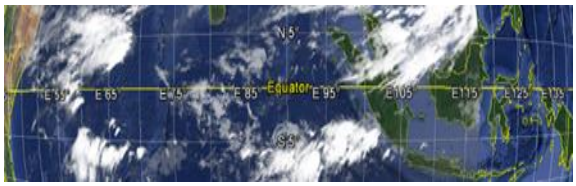

Figure 6: Earth's Grid in the Equator (Coarse-Scaled and Cartesian Form)

Figure 4 to figure 6 show the earth's grid is a kind of multi-scale and hybrid grid.

The principle of scaling up is effective areas such as wellbore or existence of fracture in the reservoir remain fine-scaled and features that these areas have cause to converge the stream lines and distance between them are reduced.

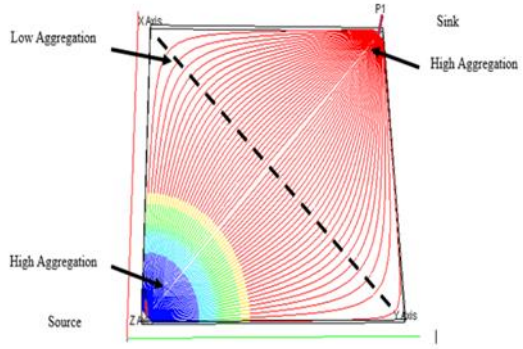

Figure 7: Source and Sink Effect of Streamline

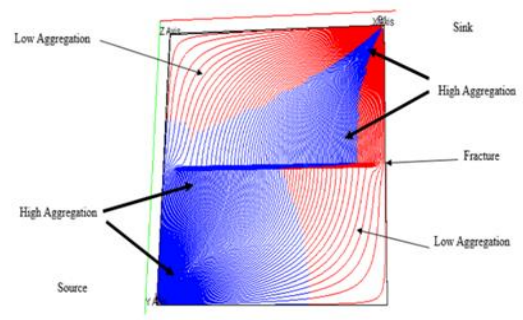

Figure 8: Source, Sink and Fracture Effect on Streamline

To implement the procedure we need a tree algorithm which consider the streamline behavior as follow:

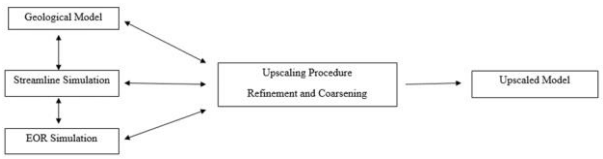

Figure 9: Tree Algorithm

The computations are required are as follow:

- Solve the pressure equation for the time step.
- Compute the total Darcy velocities based on the pressure potentials.
- Compute a set of streamlines to represent the computational domain for the saturation solver.
- Map saturations or concentrations onto the streamlines.
- Solve the saturation equation individually on each of the streamlines.
- Solve for the gravity segregation.
- Accumulate all the solution variables on each individual streamline or gravity line to form the solution on the global grid at the end of the time step.

By the means of tree algorithm for two different well patterns (Diagonal and 5-Spot) which selected for test cases the following results will be achieved (Figure 10,11).

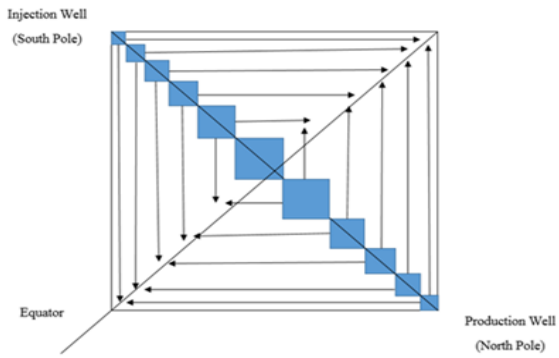

Figure 10: Diagonal Pattern

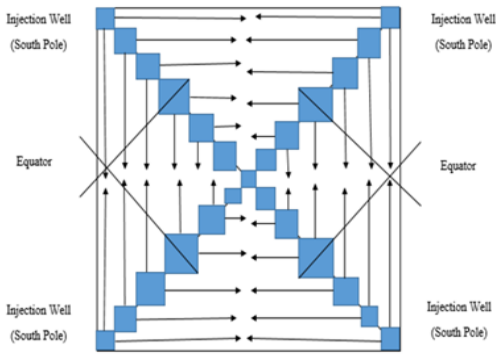

Figure 11: 5-Spot Pattern

Up-scaling studies show that past achievements require simplifying assumptions such as reservoir dimensions (1D or 2D) or the number of phases in the reservoir, which limit the effectiveness of those methods for real models. This method is independent of type of EOR method which is capable of performing on three-dimensional, heterogeneous and multiphase reservoirs and for the first time it defines a regular pattern for multi-scale grid generation.

3. Introduction of Studied Reservoir

The Reservoir has the following properties:

A 3D case with a fine mesh composed of $[40 \times 40 \times 3]$ (Total cell number: 4800). The permeability field is a distribution of high and a low values, 100 and 5 md, respectively. The porosity is constant and equal to 0.3 and initial reservoir pressure is 4011 psi.

Water Properties:

- Reference Pressure(psi): 4014.7 Psi
- Water Formation Volume Factor (bbl/STB): 1.029
- Water Compressibility: 3.13E-06
- Water Viscosity (cp): 0.31

Rock Properties:

- Reference Pressure (psi): 14.7
- Rock Compressibility: 3.0E-06
- Porosity: 0.3

Surface Densities of Reservoir Fluids (lb/ft^3):

- Oil: 49.1
- Water: 64.79
- Gas: 0.06054

Table 1: Polymer Solution Viscosity Function

The Polymer Concentration in the Solution (lb/STB)	The Corresponding Factor by Which the Water Viscosity has to be Multiplied to Give the Viscosity of the Solution
0.0	1.0
70.0	10.0

Table 2: Specifies the Polymer-Rock Properties

The Dead Pore Space for Rock Type	The Residual Resistance Factor for Rock Type	The Mass Density of Rock Type at Reservoir Condition (lb/rb)	The Adsorption index to Be Used for Rock Type
0.16	1.5	1000.0	1

Table 3: Polymer Adsorption Function

The local polymer concentration in the solution surrounding the rock (lb/STB)	The Corresponding Saturated Concentration of Polymer Adsorbed by the Rock Formation (lb/lb)
0.0	0.005
20.0	0.010
70.0	0.010

Table 4: Polymer- Salt Concentrations for Mixing Calculations

The Value of the Polymer Concentration in the Solution Which is to be Used in the Calculation of the Maximum Polymer Fluid Component Viscosity (lb/STB)	The Value of the Salt Concentration in the Solution Which is to be Used in the Calculation of the Maximum Polymer Fluid Component Viscosity (lb/STB)
50	0.0

Todd-Longstaff mixing parameter =1

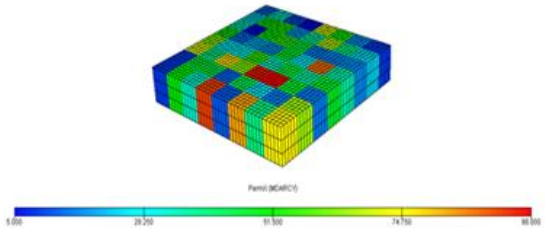

Figure 12: Permeability Map, Reservoir Dimension $[40 \times 40 \times 3]$

4. Polymer Flooding Simulation

The main objective of polymer injection during water flooding of oil reservoir is to decrease the mobility of the injected water and leading to a more efficient sweep pattern and reduced viscous fingering.

Certain plugging effects within highly permeable layers may also occur and result in the diversion of the injected water into less permeable zones of the reservoir.

The mobility decrease of injected water resulting from the addition of polymer is due to two effect:

- The viscosity of polymer solution is higher than pure water.
- The rock permeability to water is reduced after passage of a polymer solution through the rock material.

Polymer solution is often applied in the form of a tapered slug.

- At the front edge of the slug, the displacement is stable.
- At the rear edge, the mobility ratio is unfavorable and is dominated by viscous fingering.

Assumption: Temperature variation on the behavior of the polymer solution is ignored.

When a polymer solution is injected into the reservoir some of the long chain molecules constituting the polymer are adsorbed onto the rock surface.

Therefore:

- Slug width is gradually reduced in time
- Reduction in the relative permeability of polymer solution

4.1 Simulation Model

The flow of polymer solution through the porous medium is assumed to has no influence on the flow of hydrocarbon phases.

The standard black-oil equations are therefore used to describe the hydrocarbon phases in the model.

Standard water equation and additional equations are needed to describe the flow of polymer and brine within the finite difference grid.

$$\frac{d}{dt}\left(\frac{VS_w}{B_r B_w}\right) = \sum[\frac{TK_{rw}}{B_w \mu_{w\,eff} R_k}(\delta P_w - \rho_w g D_z)] + Q_w$$

Water (1)

$$\frac{d}{dt}\left(\frac{VS_w^* C_p}{B_r B_w}\right) + \frac{d}{dt}\left(V\rho_r C_a \frac{1-\emptyset}{\emptyset}\right) = \sum\left[\frac{TK_{rw}C_p}{B_w \mu_{p\,eff} R_k}(\delta P_w - \rho_w g D_z)\right] + Q_w C_p$$

Polymer (2)

$$\frac{d}{dt}\left(\frac{VS_w C_n}{B_r B_w}\right) = \sum\left[\frac{TK_{rw}C_n}{B_w \mu_{s\,eff} R_k}(\delta P_w - \rho_w g D_z)\right] + Q_w C_n$$

Brine (3)

$$S_w^* = S_w - S_{dpv} \quad (4)$$

Where

S_{dpv} : Dead pore space within each grid cell
C_a : Adsorption isotherm which is a function of the local polymer solution concentration
ρ_r : Mass density of rock formation
$\emptyset$: Porosity
ρ_w : Water density
R_k : Relative permeability reduction factor for the aqueous phase due to polymer retention
C_p , C_n : Local concentration of polymer and sodium chloride in the aqueous phase
μ_{eff} : Effective viscosity of the water, polymer and salt components
D_z : is the cell center depth

4.2 Effective Polymer Viscosity

$$\mu_{P\,,eff} = \mu_m(C_P)^{\omega}.\mu_P^{1-\omega} \quad (5)$$

Where
$\mu_m(C_P)$: Viscosity of fully mixed polymer solution as a function of polymer concentration in solution
ω : is the Todd-Longstaff mixing parameter
$\omega = 1$ means polymer solution and water mixed in each block
$\omega = 0$ means polymer solution is completely segregated from water

4.3 Effective Water Viscosity

$$\frac{1}{\mu_{w,\,eff}} = \frac{1-C}{\mu_{w,e}} + \frac{C}{\mu_{p,eff}} \quad (6)$$

Where

$$C = \frac{C_P}{C_{P,max}} \quad (7)$$

$$\mu_{w,e} = \mu_m(C_P)^{\omega}.\mu_w^{1-\omega} \quad (8)$$

C: The effective saturation for the injected polymer solution within the total aqueous phase in the cell

4.4 Permeability Reduction

The adsorption process causes a reduction in the permeability of the rock to the passage of the aqueous phase and is directly correlated with the adsorbed polymer concentration.

In order to compute the reduction in rock permeability, I need residual resistance factor (RRF) for each rock type.

$$R_k = 1 + (RRF - 1)\frac{C_a}{C_{a\,max}} \quad (9)$$

$C_{a\,max}$: Depends on rock type

4.5 Shear Thinning Effect

The shear thinning of polymer has the effect of reducing the polymer viscosity at higher flow rate.
The flow velocity is calculated as:

$$v = B_w.\frac{F_w}{\emptyset A} \quad (10)$$

Where
F_w : Water flow rate
B_w : Water formation volume factor
$\emptyset$: Average porosity of two cells
A: Flow area between two cells

5. The Procedure of Upscaling

Now we are going to define the methods used for upscaling for various parameters.

5.1 Grid Block Size

Within each coarse block the properties are simply upscaled from fine (f) to coarse (c) in a single coarse cell amalgamation $(I1, I2) \times (J1, J2) \times (K1, K2)$ as follows:

$$DX_c = \frac{\sum_f DX_f}{(J_2 - J_1 + 1)(K_2 - K_1 + 1)} \quad (11)$$

$$DY_c = \frac{\sum_f DY_f}{(I_2 - I_1 + 1)(K_2 - K_1 + 1)} \quad (12)$$

$$DZ_c = \frac{\sum_f DZ_f}{(I_2 - I_1 + 1)(J_2 - J_1 + 1)} \quad (13)$$

Where
c: Coarse
f: Fine

5.2 Renormalization Method (Upscaling for Absolute Permeability)

A way to calculate **k** is the renormalization method. Renormalization is a recursive algorithm. The effective properties of small regions of the reservoirs are first calculated and then placed on a coarse grid. The grid is further coarsened and the process repeated until a single effective property has been calculated (King *et al.*, 1993). The renormalization transformation is by no means unique and many different renormalization schemes have been proposed, some inspired by an analogy between flow in porous media, percolation processes and the flow of currents through resistors (King, 1989) (M.Babaei, 2013).

$$\mathbf{K} = f(K_1, K_2, K_3, K_4) \quad (14)$$

$$f = \frac{(2(K_1+K_2)(K_3+K_4)(K_{12}+K_{34}))}{3(K_1+K_3)(K_2+K_4)+\frac{1}{2}(K_1+K_2+K_3+K_4)(K_{12}+K_{34})} \quad (15)$$

Where
K_1, K_2, K_3, K_4: Absolute permeabilities of four constituent fine cells
K_{12}, K_{34}: Harmonic means of permeabilities of the cells with the given subscripts

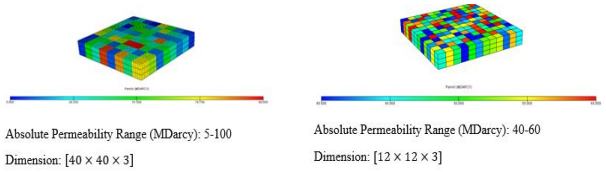

Figure 13: Implementation the Procedure of Upscaling For Absolute Permeability (Static Model)[12 × 12 × 3]

We should avoid defining too large coarse cells in order to encompass wide relative permeability variations between different rock types.

5.3 Pseudo-Function Generation

For single phase flow, permeability is assumed to be a rock property and independent of the fluids present. This is only true in the case where the rock is completely saturated with a specific fluid. In the case where two fluids are present, it is necessary to define phase specific permeabilities which are defined as the product of the absolute permeability of the rock and a function of saturation of the phase considered (M.Babaei, 2013):

$$K_l = \mathbf{K}K_{rl}(S_l) \quad (16)$$

Where
l: Phase
K_{rl}: Permeability of phase l
K: Rock permeability

Relative permeabilities are functions of saturation, implying that in the presence of more than one phase in the rock, an equation for saturation will also be needed. Assuming that a generalization of Darcy's law to multiphase flow is valid (Bear, 1972), we need to formulate equations for the flow of each phase l using relative permeabilities (M.Babaei, 2013):

$$V_l = -\frac{\mathbf{K}K_{rl}(S_l)}{\mu_l}(\nabla p_l + \rho_l g \nabla z) \quad (17)$$

Where
V: Volumetric flow
p: Pressure
g: Gravitational Force
z: Spatial coordinate

A common approach is to use an averaging technique to generate relative permeability curves similar to global-local upscaling. For instance, for calculating an upscaled mobility of phase l, denoted by λ_l^* , a fine scale global solution, provides the flow rate between the grid blocks. To match the phase flow rates between coarse grid blocks E_i and E_j in x direction the following must hold:

$$\sum_{K=1}^{N}(f_l)_k = \overline{f}_l \quad (18)$$

Substituting in Darcy's law for multiphase flow:

$$-\sum_{K=1}^{N}(t\lambda_l(S)\nabla p)_K = -(T^*\lambda_l^*(\overline{S})\overline{\nabla p})_{ij} \quad (19)$$

Where
t: Fine transmissibility
T^*: Coarse transmissibility

The upscaling for transmissibilities is achieved as a simple average. Between the centers of two neighboring coarse cells, $TRANX_C$ $(Coarse\ Transmissibility\ in\ X-direction)$is obtained from a harmonic average of $TRANX_f(Fine\ transmissibility\ in\ X-direction)$in the X-direction and by summing in the Y and Z directions so that:

$$TRANX_c = \sum_J \sum_K \left[\frac{1}{\sum_I \left[\frac{1}{TRANX_f}\right]}\right] \quad (20)$$

5.4 Volume Average Equations

The pore volume of a refined global cell may differ from the sum of the pore volumes of the local cells which it contains, either because the local porosities

and net-to-gross ratios differ from the values for the host cell or because of discrepancies in geometry. After computing the local pore volumes, replaced the pore volume of the host cell with the sum of the refined pore volumes.

c: Coarse
f: Fine
PV: Pore Volume

$$PV_c = \sum_f PV_f \quad (21)$$

6. Test Cases

In this section, different cases like diagonal and 5-spot well pattern and a fractured reservoir are presented to test the inspired by nature upscaling approach.

6.1 Reservoir with one injection and production well (Diagonal Pattern)

The first case in this study corresponds to a 3D case with a fine mesh composed of 40 by 40, 4800 cells with three layers and a coarse mesh of 12 by 12 cells. The range of permeability field is a distribution of high and a low values, 100 and 5 md (For fine model), respectively and for upscaled model 60 and 40 md. The porosity is constant and equal to 0.3. Water is injected at one corner of the model at a rate of 200 STB/day, and the fluid is produced at the opposite corner. The concentration of polymer in the injection stream for injection well is 50 lb/STB. Simulation Duration, 1700 days.

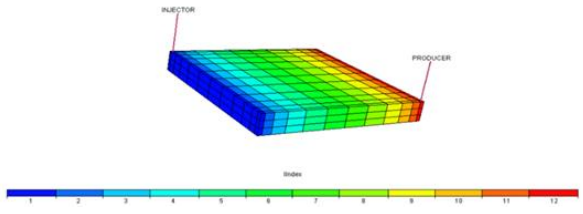

Figure 14: Upscaled View of the Reservoir with one Injection and Production Well

6.2 5-Spot Pattern

The second case in this study corresponds to a 3D case with a fine mesh composed of 40 by 40 , 4800 cells with three layers and a coarse mesh of 16 by 16 cells . The range of permeability field is a distribution of high and a low values, 100 and 5 md (For fine model), respectively and for upscaled model 60 and 40 md. The porosity is constant and equal to 0.3. Water is injected at four corners of the model at a rate of 200 STB/day for each injection well, and the fluid is produced at the center of model. The concentration of polymer in the injection stream for each injection well is 50 lb/STB. Simulation Duration, 1700 days.

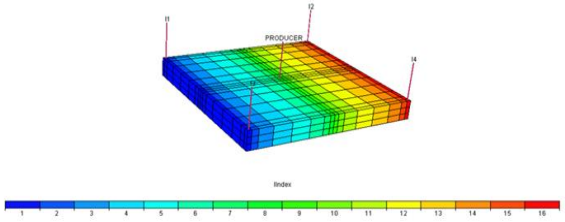

Figure 15: Upscaled View of the Reservoir in 5-Spot Pattern

7. Numerical Results

In this section we investigated the result of algorithm defined previous .The different scenarios defined as below:

- Fine Model: Fine and heterogeneous model with 3 layers and 4800 cells.
- UPIN: A multiphase upscaling method which inspired by Earth's grid and able to identify places with high permeability based on the behavior of flow lines (frontsim) and perform in each layer in vertical direction.
- UPIN(CW),UPIN(RW): In order to enhance resolution around significant regions in different geometries (Cartesian and Radial) these scenarios defined.

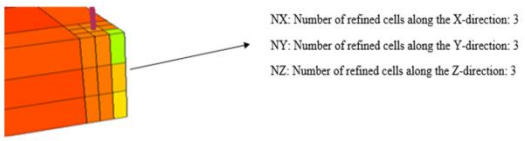

Figure 16: Local Grid Refinement (LGR) around the Production Wellbore in Cartesian Coordinate, UPIN(CW), Increasing the Resolution around the Production Well For Diagonal Pattern

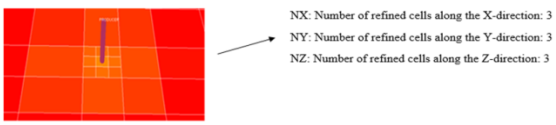

Figure 17: Local Grid Refinement (LGR) around the Production Wellbore in Cartesian Coordinate, UPIN(CW), Increasing the Resolution around the Production Well For Diagonal Pattern For 5-Spot Pattern

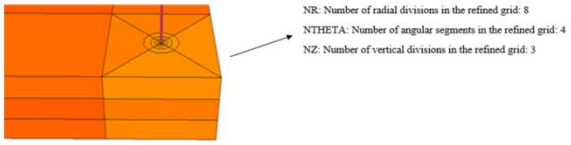

Figure 18: Local Grid Refinement (LGR) around the Production Wellbore in Radial Coordinate (Hybrid Grid), UPIN (RW), Increasing the Resolution around the Production Well For Diagonal Pattern

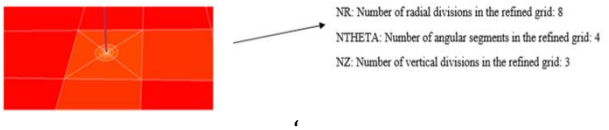

Figure 19: Local Grid Refinement (LGR) around the Production Wellbore in Radial Coordinate (Hybrid Grid), UPIN (RW), Increasing the Resolution around the Production Well For 5-Spot Pattern

First of all need to choose the solver method (Fully Implicit or IMPES) for fine model and choose one of them base on minimum elapse time, in three different cases we investigated fully implicit was faster enough in compare with IMPES method therefore, we selected fully implicit as our solver method.

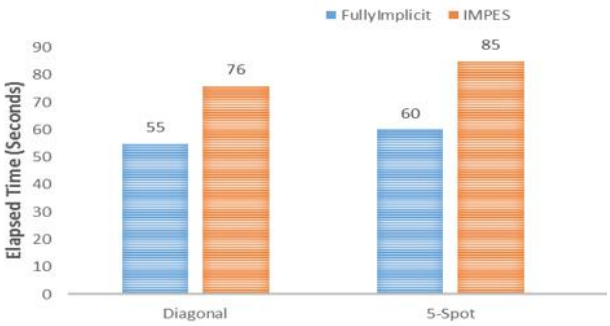

Figure 20: Elapsed Time for Fine Model in Two Different Methods

7.1 Reservoir with one injection and production well (Diagonal Pattern)

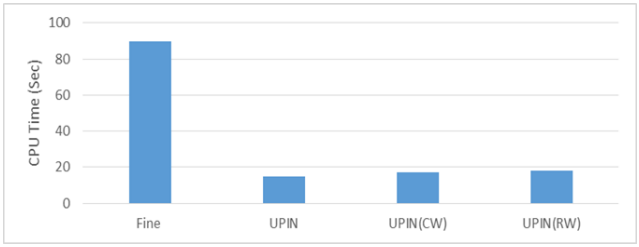

Figure 21: CPU Time

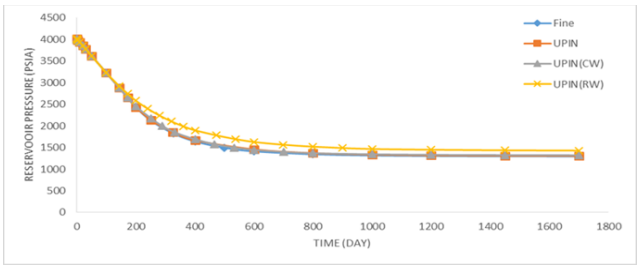

Figure 22: Reservoir Pressure

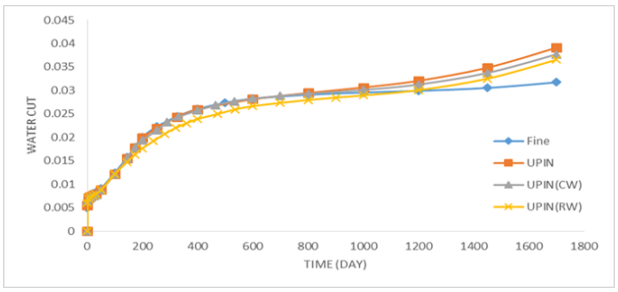

Figure 23: Water Cut

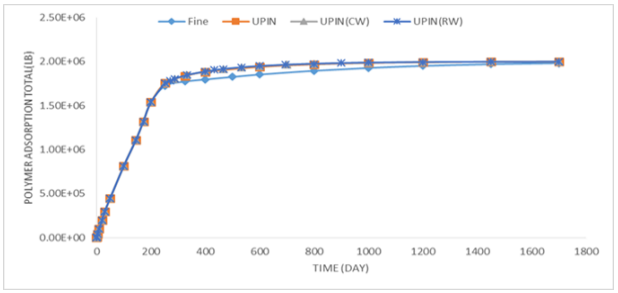

Figure 24: Polymer Adsorption Total

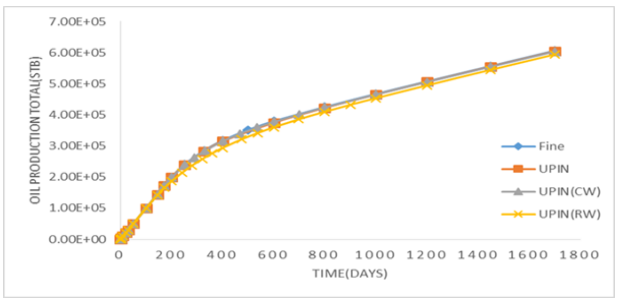

Figure 25: Oil Production Total

7.2 5-Spot Pattern

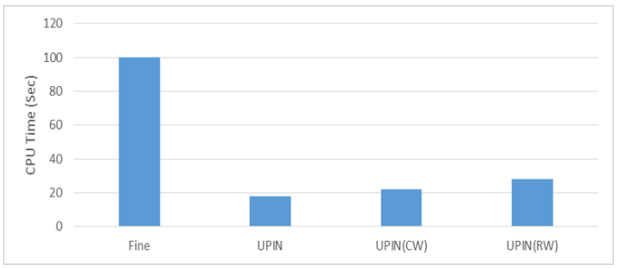

Figure 26: CPU Time

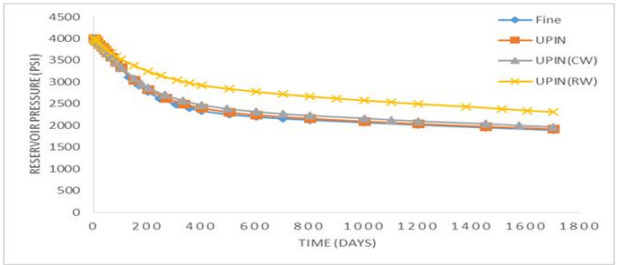

Figure 27: Reservoir Pressure

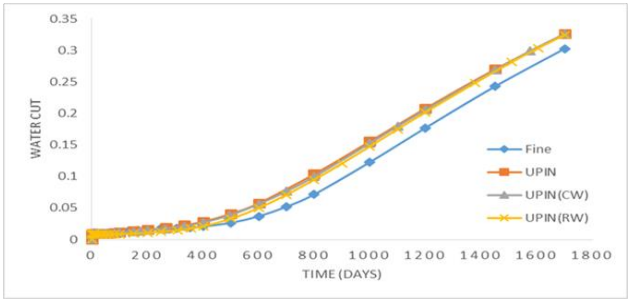

Figure 28: Water Cut

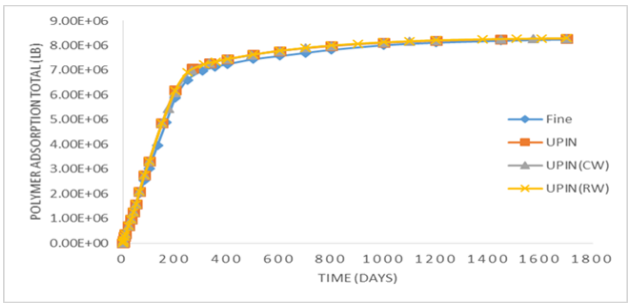

Figure 29: Polymer Adsorption Total

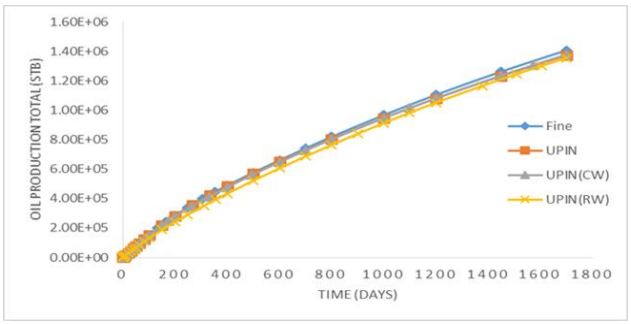

Figure 30: Oil Production Total

Now comparison of different scenario in different aspect with the fine model.

Table 5: CPU Time

	UPIN	UPIN(CW)	UPIN(RW)
Reservoir with one injection and Production Well	6 Times faster than fine model	5.29 times faster than fine model	5 Times faster than fine model
5-Spot	5.5	4.54	3.57

Table 6: Reservoir Pressure (Percentage Error)

	UPIN	UPIN(CW)	UPIN(RW)
Reservoir with one injection and Production Well	0.83%	2.11%	10.35%
5-Spot	1.16%	3.88%	21.91%

Table 7: Water Cut (Percentage Error)

	UPIN	UPIN(CW)	UPIN(RW)
Reservoir with one injection and Production Well	11.76%	10%	15.15%
5-Spot	7.71%	7.81%	7.23%

Table 8: Polymer Adsorption Total (Percentage Error)

	UPIN	UPIN(CW)	UPIN(RW)
Reservoir with one injection and Production Well	0.85%	0.91%	1.2%
5-Spot	0.46%	0.08%	0.6%

Table 9: Oil Production Total (Percentage Error)

	UPIN	UPIN(CW)	UPIN(RW)
Reservoir with one injection and Production Well	0.28%	0.47%	2%
5-Spot	2.47%	2.09%	3.69%

8. Summery of Results

Around the production well because of the high volume of computing, the excessive resolution, in addition to increasing the time of the calculation, even leads to errors.

Unstructured grid modeling which allows the definition of composite grid due to the conversion of various parameters the accuracy of this grid modeling is not as high as the geological model (figure 31).

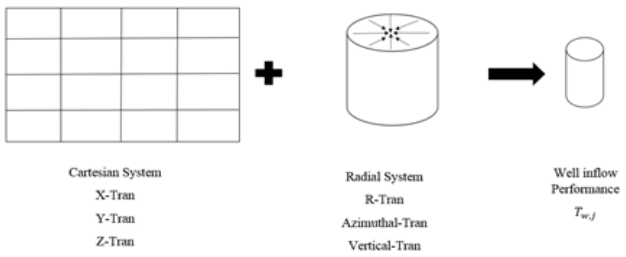

Figure 31: Composite Grid

References

Mohammad Reza Rasaei · Muhammad Sahimi , "Upscaling and Simulation of Waterflooding in Heterogeneous Reservoirs Using Wavelet Transformations: Application to the SPE-10 Model, 20 July 2007.

Masoud Babaei, Multiscale Wavelet and Upscaling-Downscaling for Reservoir Simulation, January 2013.

An Introduction to Reservoir Simulation Using MATLAB , SINTEF ICT, Department of Applied Mathematics , May 27, 2014 Oslo, Norway.

F. Brezzi and M. Fortin. Mixed and Hybrid Finite Element Methods, volume 15 of Springer Series in Computational Mathematics. Springer Verlag, New York, 1991. ISBN 0-387-97582-9.

J. E. Aarnes, S. Krogstad, and K.-A. Lie. Multiscale mixed/mimetic methods on corner-point grids. Comput. Geosci., 12(3):297-315, 2008. ISSN 1420-0597.

F. Brezzi, K. Lipnikov, and V. Simoncini. A family of mimetic finite difference methods on polygonial and polyhedral meshes. Math. Models Methods Appl. Sci., 15:1533-1553, 2005.

M. A. Christie and M. J. Blunt. Tenth SPE comparative solution project: A comparison of upscaling techniques. SPE Reservoir Eval. Eng., 4:308-317, 2001.

Y. Efendiev and T. Y. Hou. Multiscale Finite Element Methods, volume 4 of Surveys and Tutorials in the Applied Mathematical Sciences. Springer Verlag, New York, 2009.

D. W. Peaceman. Fundamentals of Numerical Reservoir Simulation. Elsevier Science Inc., New York, NY, USA, 1991. ISBN 0444415785.

D. K. Ponting. Corner point geometry in reservoir simulation. In P. King, editor, Proceedings of the 1st European Conference on Mathematics of Oil Recovery, Cambridge, 1989, pages 45-65, Oxford, July 25-27 1989. Clarendon Press.

M. Prevost, M. Edwards, and M. Blunt. Streamline tracing on curvilinear structured and unstructured grids. SPE J., 7(2):139-148, June 2002.

Aasum, Y., Kasap, E., Kelkar, M.: "Analytical Upscaling of Small-Scale Permeability Using a Full Tensor", Paper SPE 25913 presented at the SPE Rocky Mountain Regional/Low Permeability Reservoirs Symposium held in Denver, CO, April 12-14, 1993.

Barker, J.W., Thibeau, S.: "A Critical Review of the Use of Pseudo Relative Permeabilities for Upscaling", Paper SPE 35491 presented at European 3-D Reservoir Modeling Conference held in Stavanger, Norway, April 16-17, 1996.

Bedrikovetsky, P.G., Potsch, K.T., Polyanin, A.D., Zhurov, A.I.: "Upscaling of the Water flood Reservoir Properties on the Core Level: Laboratory Study, Macro and Micro Modeling", Paper SPE 29870 presented for SPE Middle East Oil Show held in Bahrain, March 11-14, 1995.

Coll, C., Muggeridge, A.H., Jing,, X.D.: "Regional Upscaling: A New Method to Upscale Waterflooding in Heterogeneous Reservoirs for a Range of Capillary and Gravity Effects", Paper SPE 59337 presented at 2000 SPE/DOE Improved Oil Recovery Symposium held in Tulsa, OK, April 3-5, 2000.

Craft, B.C., Hawkins, M.F.: Applied Reservoir Engineering, Prentice Hall, 1990.

Demin, W., Jiecheng, C., Qingyan, Y. *et al*. 2000. Viscous-Elastic Polymer Can Increase Microscale Displacement Efficiency in Cores. Presented at the SPE Annual Technical Conference and Exhibition, Dallas, Texas, 1-4 October 2000. SPE-63227-MS.

Herr, J.W. and Routson, W.G. 1974. Polymer Structure and Its Relationship to the Dilute Solution Properties of High Molecular Weight Polyacrylamide. Presented at the Fall Meeting of the Society of Petroleum Engineers of AIME, Houston, Texas, 6-9 October 1974. SPE-5098-MS.

Stahl, G.A., Moradi-Araghi, A., and Doe, P.H. 1988. High Temperature and Hardness Table 14. Copolymers of Vinylpyrrolidone and Acrylamide. In Water-Soluble Polymers for Petroleum Recovery, G.A. Stahl and D.N. Schulz eds., 121-130. New York and London: Plenum Press.

Duda, J.L., Klaus, E.E., and Fan, S.K. 1981. Influence of Polymer-Molecule/Wall Interactions on Mobility Control. Society of Petroleum Engineers Journal 21 (5): 613-622. SPE-9298-PA.

Flory, P.J. 1953. Principles of Polymer Chemistry. Ithaca, New York: Cornell U. Press.

Gogarty, W.B. 1967. Mobility Control with Polymer Solutions. SPE J. 7 (2): 161–173. SPE-1566-PA.

DeHekker, T.G., Bowzer, J.L., Coleman, R.V. *et al*. 1986. A Progress Report on Polymer-Augmented Waterflooding in Wyoming's North Oregon Basin and Byron Fields. Presented at